Neutral particle emission of the PULSATOR plasma

A.I. Kislyakov*
H.M. Mayer
W. Ott
F. Wagner

IPP 2/230
IPP III/25

July 1976

MAX-PLANCK-INSTITUT FÜR PLASMAPHYSIK

8046 GARCHING BEI MÜNCHEN

MAX-PLANCK-INSTITUT FÜR PLASMAPHYSIK

GARCHING BEI MÜNCHEN

Neutral particle emission of the PULSATOR plasma

A.I. Kislyakov*
H.M. Mayer
W. Ott
F. Wagner

IPP 2/230
IPP III/25

July 1976

* A.F. Ioffe Physico-Technical Institute
of the Academy of Sciences of the USSR,
Leningrad

IPP 2/230
IPP III/25

Neutral particle emission of the PULSATOR plasma

A. I. Kislyakov
H.M. Mayer
W. Ott
F. Wagner

July 1976

Abstract

The energy distribution function of the neutral particles emitted from the PULSATOR tokamak plasma was determined absolutely and compared with theoretical results obtained with the Duechs code.

INTRODUCTION

An important method of determining the ion temperature of a laboratory plasma is the analysis of the spectrum of fast neutrals. They are created in the plasma by charge exchange collisions between the ions and the background neutrals. A five-channel energy analyzer for neutral particles /1/ which was constructed at the Ioffe Technical Institute in Leningrad was installed on top of the PULSATOR tokamak as shown in Fig. 1. In a first series of measurements the energy distribution of the emitted neutrals was determined when PULSATOR was operated in the high-density regime /2/. The addition of gas during the discharge increased the electron density in the plasma above 10^{14} cm^{-3}. The increase of the ion temperature with the rising plasma density could clearly be seen in our measurements. In this report we only want to describe the measurement of the neutral particle flux and compare it with the flux spectrum as calculated by Duechs /3, 4/. The interpretation of the measured flux spectrum as an independent means of determining the ion temperature in the plasma will be treated in a separate report /5/.

MEASUREMENTS AND COMPARISON WITH THEORY

For the absolute measurement of the neutral particle flux two different techniques were employed in parallel: particle counting and current measurement. In counting techniques it is common practice to distinguish signal pulses from noise pulses by accepting only those pulses which surpass a voltage threshold U_o. U_o can be deduced from the dependence of the counting rate N on the threshold voltage U of the discriminator. This dependence was exponential in our case:

$$N \propto \exp(-U/2U_o)$$

For the determination of U_0 a built-in alkali ion source was used. The correlation coefficient between the current and counting rate was given by the amplification of the particle detector and had to be determined separately for each multiplier. This coefficient was obtained by measuring the number of impinging particles during a discharge in a pre-set time interval and comparing this figure with the current produced by the same number of ions in the same time interval in the next discharge. The plasma discharges were sufficiently reproducible for this purpose.

The energy distribution of the flux of neutral particles emitted from the plasma is deduced from

$$\frac{d\Phi}{dE} = \frac{dN}{dt} \quad \frac{d\Omega \; dF}{\Delta E \cdot c \; (E)}$$

where dN/dt is the measured particle rate, Δ E is the half-width of a channel, being obtained by a separate calibration with the built-in ion source. c(E) is the detection efficiency for neutrals as measured at the Ioffe Institute at Leningrad and $d\Omega \; dF$ is the acceptance of the analyzer ($6 \cdot 10^{-6}$ cm^2 sterad) given by the entrance and exit slits of the system.

The measurements were carried out during a series of "standard" discharges which were reproducible from shot to shot. It was hereby possible to determine the neutral-particle spectrum over a wide energy range. The results are shown in Figs. 3a-c and 4a-c. In these figures the same experimental results are compared with the results of two computer runs differing in the assumed time dependence of the pulsed neutral gas influx and in the coefficient R for the recycling of particles impinging on the walls. The first calculation uses R = 1 and an additional influx according to curve 1 of Fig. 2. It leads to the curves of Figs. 3a-c. The second calculation uses R = 0.96, an additional influx according to curve 2 of Fig. 2, and yields the curves of Figs. 4a-c.

DISCUSSION

A comparison of Figs. 3a-c with Figs. 4a-c shows that the differences between the two computer runs are relatively small. At 60 ms and 80 ms, when the plasma densities are around $1 \cdot 10^{14}$ cm^{-3}, there is a surprising overall agreement between measurements and calculation. The agreement is within a factor of 2 over a flux range of three orders of magnitude. Only at lower energies ($E < 500$ eV) are the experimental points clearly below the calculated curves. This disagreement may be connected with the tendency of the computer simulation to overemphasize the outer layers, thus giving rise to enhanced flux in the lower energy range. On the other hand, the calibration of the analyzer becomes increasingly difficult at the lower end of the energy spectrum.

In contrast to the relatively good agreement for the high densities, there is a clear discrepancy between experiment and theory at low densities. This can be seen in Figs. 3c and 4c. (At 40 msec the additional gas influx has not yet noticeably influenced the discharge.) The slope of the experimental points this time is about half the slope of the theoretical curves. This means that the experimental ion temperature is about twice the theoretical one. This discrepancy is due to the role of impurities in the discharge, which is underestimated when the computer simulation of the high-density discharge is applied to the low-density regime /6/.

ACKNOWLEDGEMENT

These measurements were carried out within the PULSATOR group. The authors wish to thank D. Duechs for making available to them the results of his calculations and for discussions, E. Speth for cooperation in the preparatory stage of the experiment and E. Held for technical assistance.

REFERENCES

/1/ W.W. Afrosimov, E.L. Beresovski, I.P. Gladkovski, A.I. Kislyakov, M.P. Petrov, W.A. Sadovnikov: Zh.T.F 45, 56 (1975), English translation: Soviet Physics - Technical Physics 20, 33 (1975)

/2/ O. Klüber et al.: Nuclear Fusion 15, 1194 (1975)

/3/ D.M. Meade, H.P. Furth, P.H. Rutherford, F. Seidl, D.F. Duechs, Proc. Vth Int. Conf. on Plasma Physics and Controlled Nuclear Fusion Research, Tokyo, Nov. 1974, IAEA Vienna, 1975, Vol. I, p. 605

/4/ D.F. Düchs; IPP Laboratory Report in preparation

/5/ H.M. Mayer, IPP Laboratory Report in preparation

/6/ D.F. Düchs: private communication

Fig. 1

a) Schematic cross-section in a poloidal plane. The angle between the beam axis and the normal to the assumed plasma surface was $\alpha = 11^{\circ}$.

b) Schematic cross-section of the equatorial plane of PULSATOR, R = 70 cm, a = 11 cm.

Fig. 2 Time dependence of the pulsed gas inflow as assumed in two different calculations

Fig. 3a-c Measured and calculated flux spectra at 3 stages of the discharge. The calculated discharge parameters are shown as inserts. The calculations assume gas inflow as in curve 1 of Fig. 2

Fig. 4a-c As in Figs. 3a-c, however, calculations made with gas inflow according to curve 2 of Fig. 2

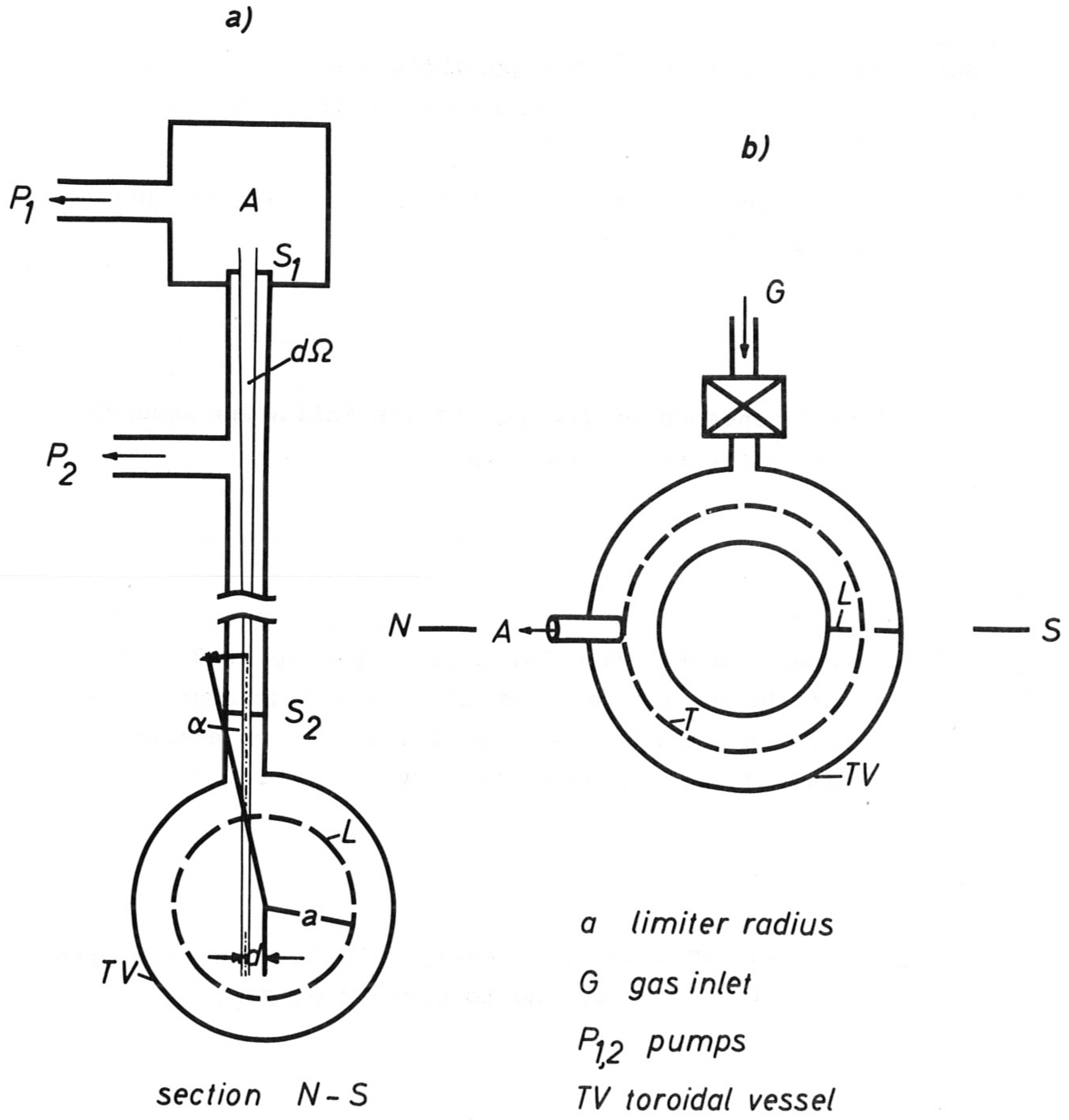

section N - S

A	analyzer
$S_{1,2}$	diaphragms
dΩ	solid angle
L	limiter
a	limiter radius
G	gas inlet
$P_{1,2}$	pumps
TV	toroidal vessel
T	toroidal axis
α	inclination of beam to surface normal
d	distance beam axis to toroidal axis

Fig. 1

Fig. 2

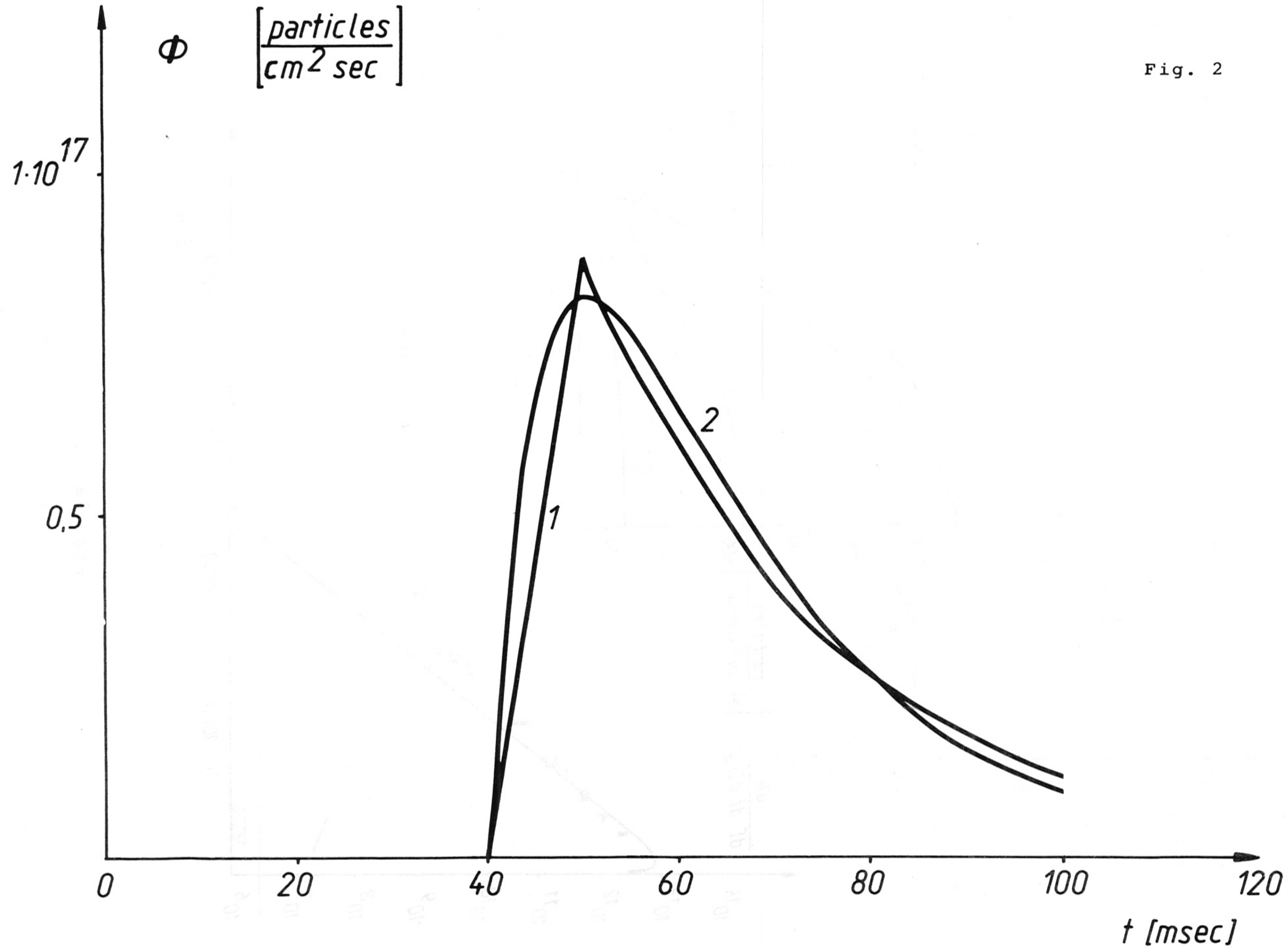

Φ $\left[\frac{\text{particles}}{\text{cm}^2\ \text{sec}}\right]$
$1\cdot10^{17}$
0,5
0
20
40
60
80
100
120
t [msec]
1
2

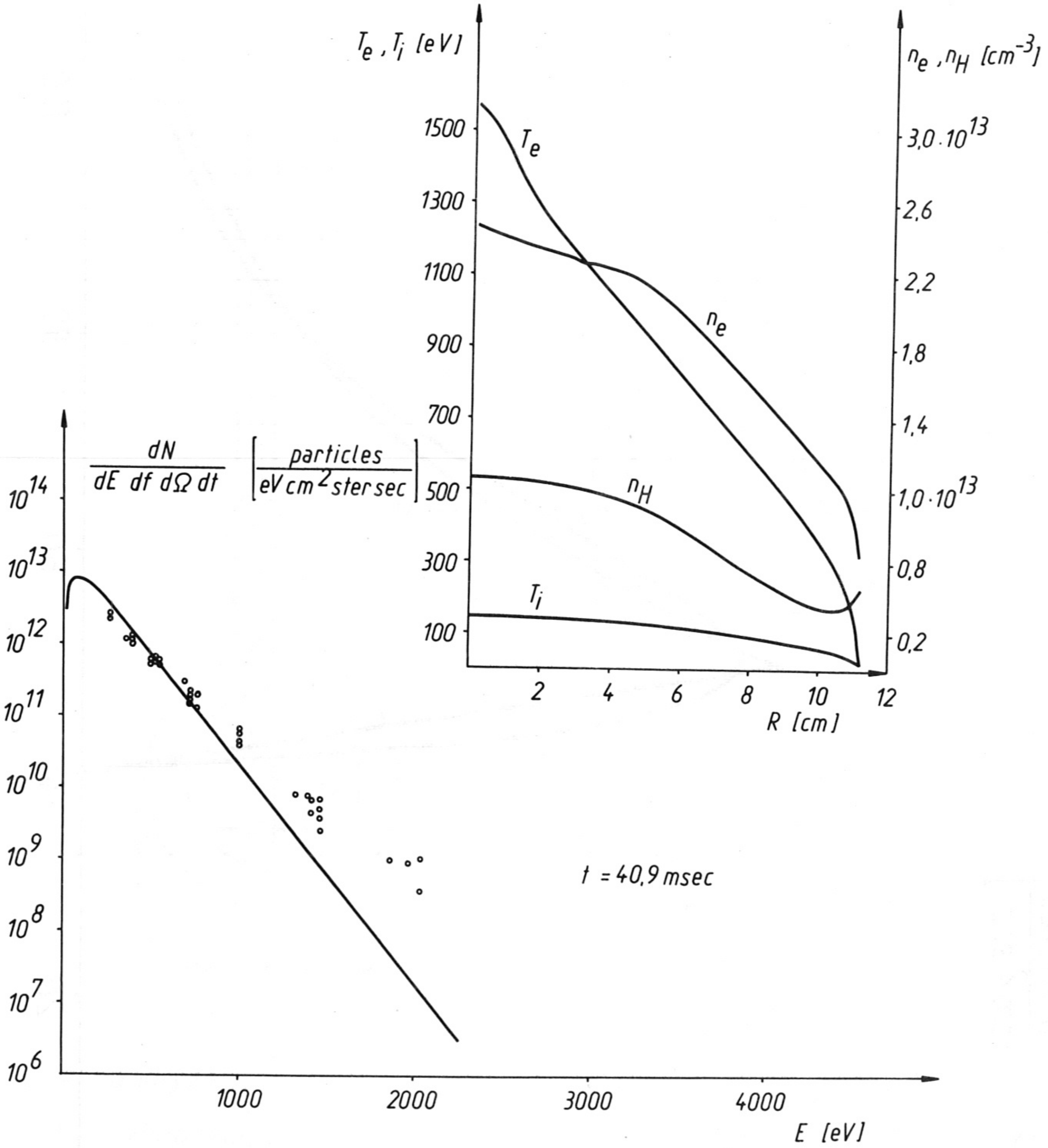
T_e, T_i [eV]
1500
1300
1100
900
700
500
300
100
n_e, n_H [cm^{-3}]
$3{,}0 \cdot 10^{13}$
2,6
2,2
1,8
1,4
$1{,}0 \cdot 10^{13}$
0,8
0,2
T_e
n_e
n_H
T_i
2
4
6
8
10
12
R [cm]
$\frac{dN}{dE\, df\, d\Omega\, dt}$ $\left[\frac{\text{particles}}{\text{eV cm}^2 \text{ster sec}}\right]$
10^{14}
10^{13}
10^{12}
10^{11}
10^{10}
10^{9}
10^{8}
10^{7}
10^{6}
1000
2000
3000
4000
E [eV]
t = 40,9 msec

Fig. 3a

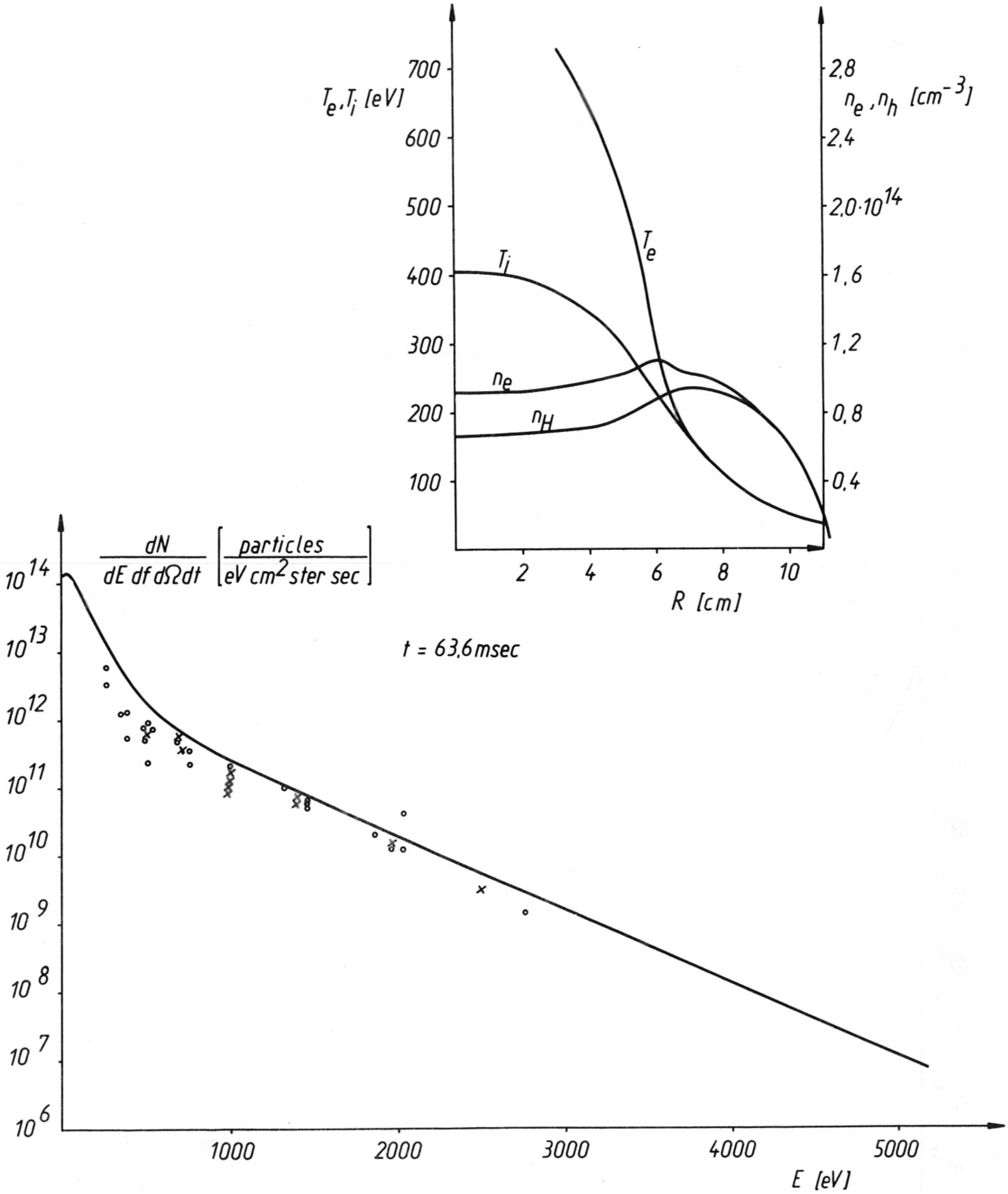
T_e, T_i [eV]
700
600
500
400
300
200
100
T_i
T_e
n_e
n_H
n_e, n_h [cm^{-3}]
2,8
2,4
$2,0 \cdot 10^{14}$
1,6
1,2
0,8
0,4
2
4
6
8
10
R [cm]
$\frac{dN}{dE\, df\, d\Omega\, dt}$ $\left[\frac{\text{particles}}{\text{eV cm}^2\text{ ster sec}}\right]$
10^{14}
10^{13}
10^{12}
10^{11}
10^{10}
10^{9}
10^{8}
10^{7}
10^{6}
t = 63,6 msec
1000
2000
3000
4000
5000
E [eV]

Fig. 3b

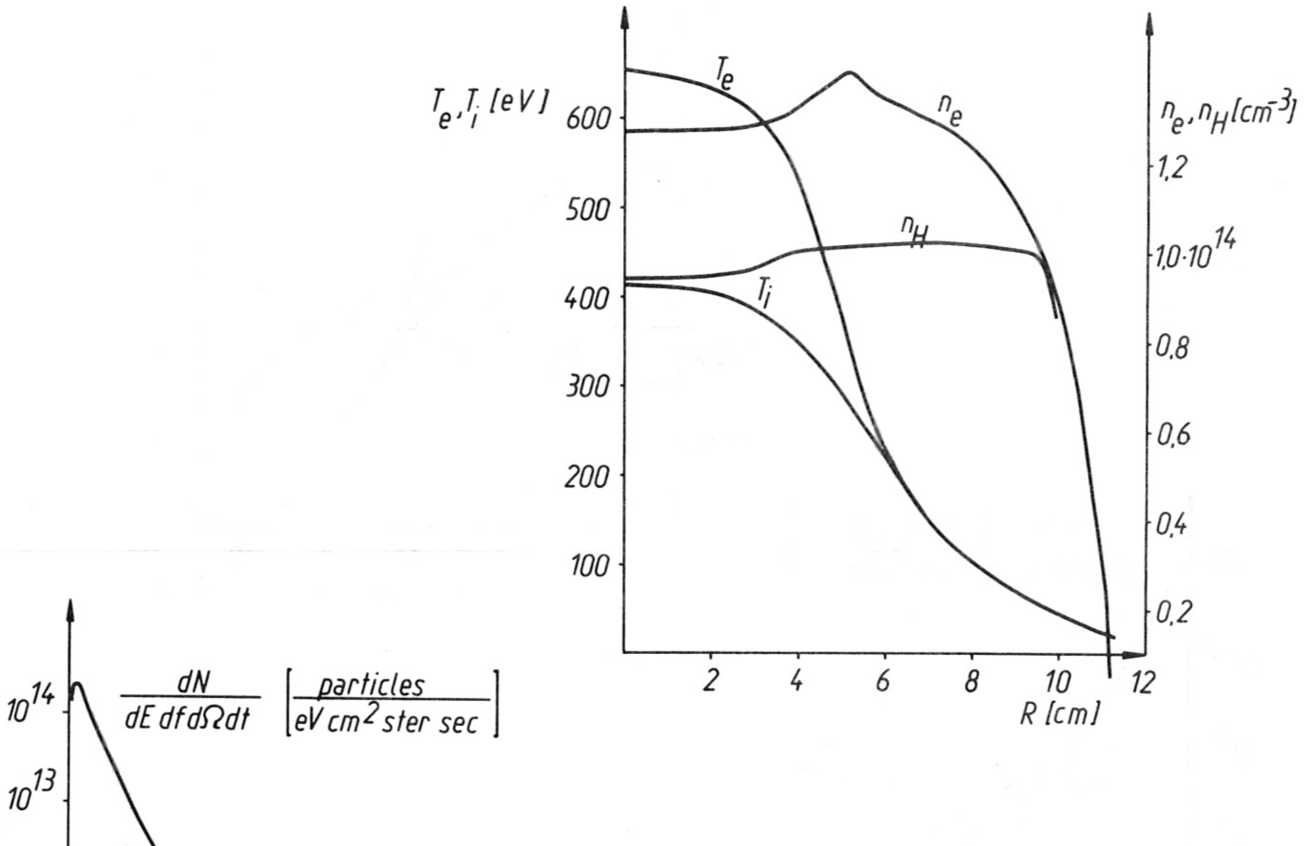
T_e, T_i [eV]
600
500
400
300
200
100
T_e
T_i
n_e
n_H
n_e, n_H [cm^{-3}]
1,2
$1{,}0 \cdot 10^{14}$
0,8
0,6
0,4
0,2
2
4
6
8
10
12
R [cm]
$\frac{dN}{dE\, df\, d\Omega\, dt}$ $\left[\frac{particles}{eV\, cm^2\, ster\, sec}\right]$
10^{14}
10^{13}
10^{12}
10^{11}
10^{10}
10^{9}
10^{8}
10^{7}
10^{6}
t = 77,8 msec
1000
2000
3000
4000
E [eV]

Fig. 3c

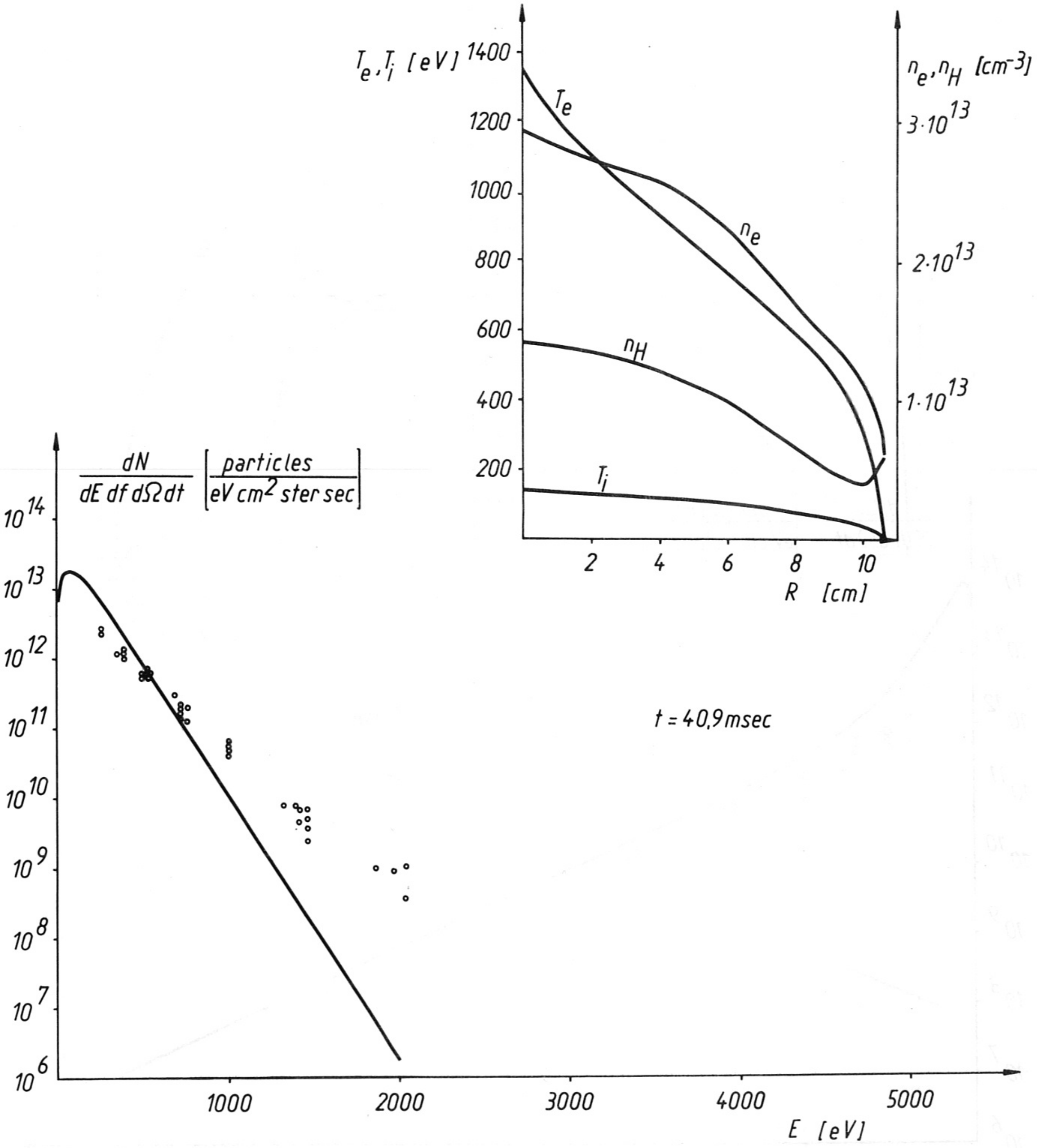
T_e, T_i [eV]
1400
1200
1000
800
600
400
200
T_e
n_e
n_H
T_i
n_e, n_H [cm^{-3}]
$3 \cdot 10^{13}$
$2 \cdot 10^{13}$
$1 \cdot 10^{13}$
2
4
6
8
10
R [cm]
t = 40,9 msec
$\frac{dN}{dE\, df\, d\Omega\, dt}$ $\left[\frac{particles}{eV\, cm^2\, ster\, sec}\right]$
10^{14}
10^{13}
10^{12}
10^{11}
10^{10}
10^{9}
10^{8}
10^{7}
10^{6}
1000
2000
3000
4000
5000
E [eV]

Fig. 4a

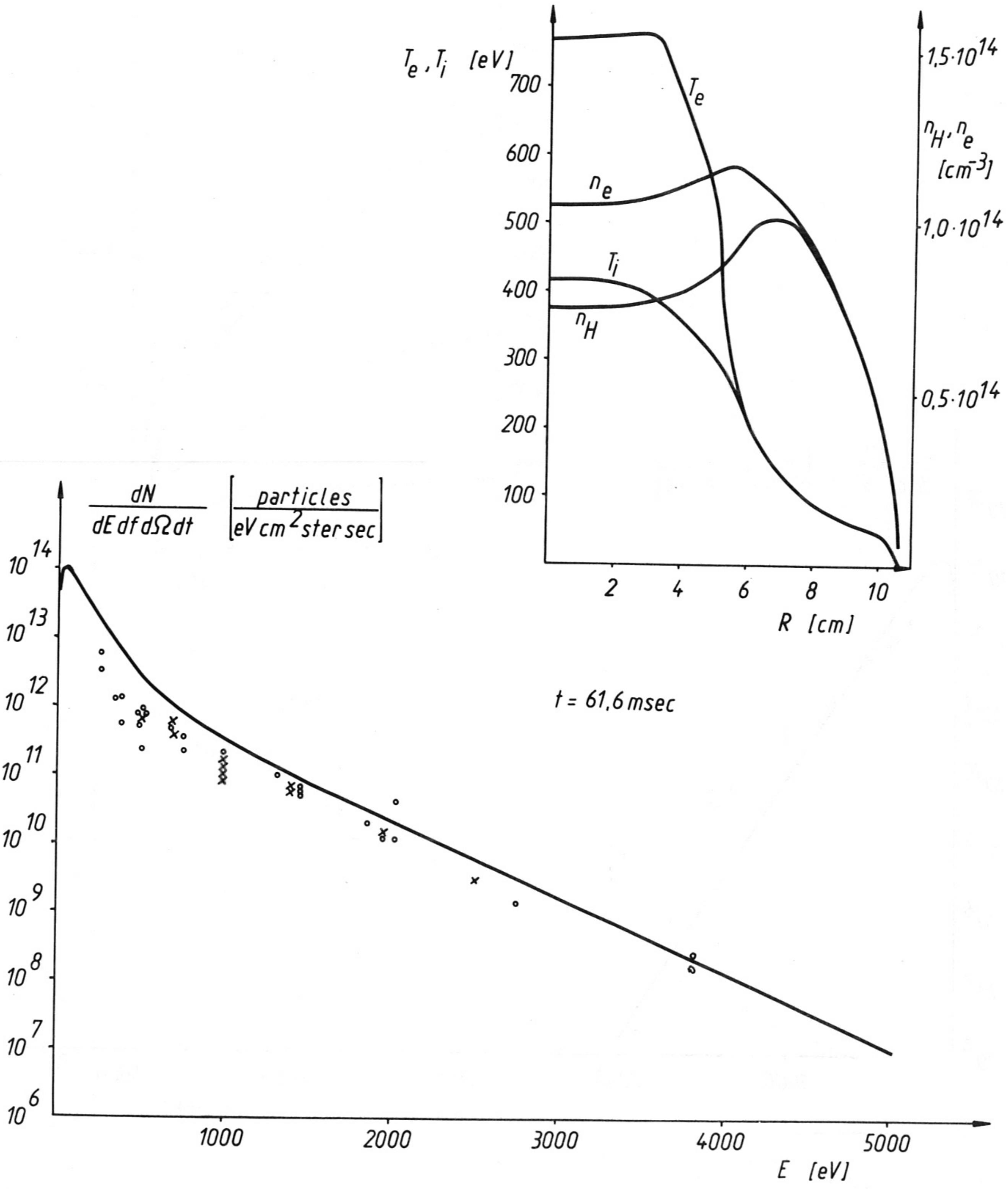

t = 61,6 msec

Fig. 4b

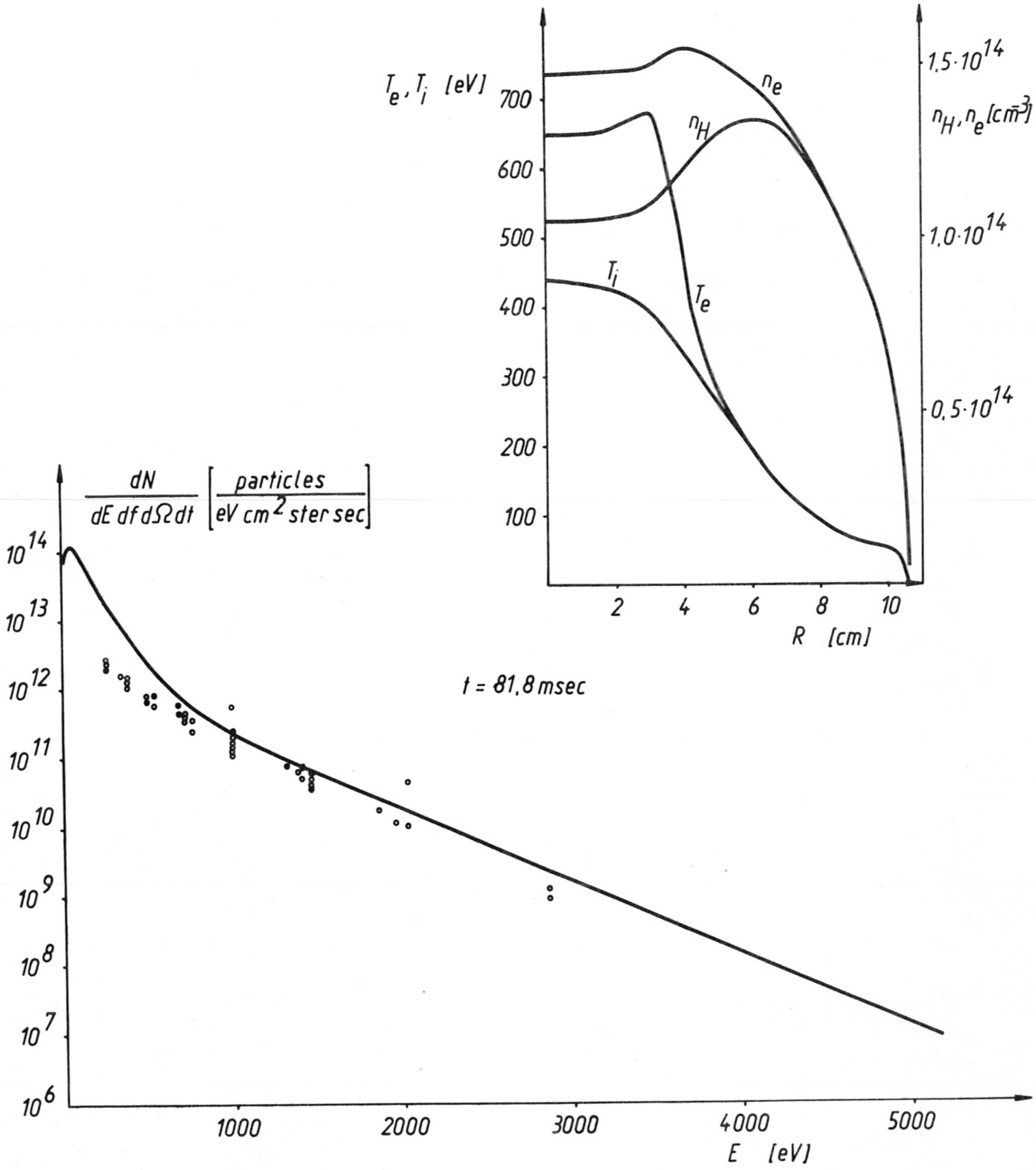T_e, T_i [eV]
700
600
500
400
300
200
100
$1,5 \cdot 10^{14}$
$n_H, n_e [cm^{-3}]$
$1,0 \cdot 10^{14}$
$0,5 \cdot 10^{14}$
n_e
n_H
T_i
T_e
2
4
6
8
10
R [cm]
t = 81,8 msec
$\frac{dN}{dE\,df\,d\Omega\,dt} \left[\frac{particles}{eV\,cm^2\,ster\,sec}\right]$
10^{14}
10^{13}
10^{12}
10^{11}
10^{10}
10^{9}
10^{8}
10^{7}
10^{6}
1000
2000
3000
4000
5000
E [eV]

Fig. 4c